A qubit coupled with confined phonons: the interplay between true and fake decoherence.

Vincent Pouthier*
Institut UTINAM, Université de Franche-Comté, CNRS UMR 6213, 25030 Besançon Cedex, France
(Dated: May 24, 2013)

The decoherence of a qubit coupled with the phonons of a finite-size lattice is investigated. The confined phonons no longer behave as a reservoir. They remain sensitive to the qubit so that the origin of the decoherence is twofold. First, a qubit-phonon entanglement yields an incomplete true decoherence. Second, the qubit renormalizes the phonon frequency resulting in fake decoherence when a thermal average is performed. To account for the initial thermalization of the lattice, the quantum Langevin theory is applied so that the phonons are viewed as an open system coupled with a thermal bath of harmonic oscillators. Consequently, it is shown that the finite lifetime of the phonons does not modify fake decoherence but strongly affects true decoherence. Depending on the values of the model parameters, the interplay between fake and true decoherence yields a very rich dynamics with various regimes.

PACS numbers:

I. INTRODUCTION

Modeling the exciton dynamics is a key issue for understanding transport phenomena in molecular lattices[1–3]. For instance, in light-harvesting complexes[4,5], dendrimers[6,7] and polymers[8,9], Frenkel excitons participate in the conversion of electromagnetic energy into chemical energy. In α-helices, amide-I vibrons play a key role in the transduction of the chemical energy into mechanical work[10–15]. In adsorbed nanostructures, vibron transport competes with nanoscale electronics[16–21] and is a promising way for quantum information processing[22,23].

In such lattices, atomic subunits occupy sites regularly distributed so that the exciton accounts for the coherent delocalization of an electronic transition or a high-frequency vibrational mode. However, it does not propagate freely but interacts with the phonons of the host medium[24,25]. In an infinite lattice, the phonons behave as a reservoir[26] responsible for quantum decoherence[27,28]. They induce random fluctuations of the excitonic energies so that dephasing-limited coherent dynamics arises.

Recently[29–32], the exciton-phonon problem was revisited to account for finite-size effects. In a confined lattice, the phonons no longer form a reservoir[33]. Their dynamics exhibits quantum recurrences and memory effects so that a strong non-markovian regime occurs[34]. The correlations between the exciton and the phonons cannot be neglected during the propagation. Consequently, generalized master equation approaches break down within the Born approximation[35].

Although many strategies exist to overcome such problems[36–40], we have developed a quite powerful unitary transformation-based method[29–32]. Within this method, the exciton and the phonons are treated on an equal footing to estimate the system eigenstates and to go beyond the Born approximation. It was shown that a dual dressing mechanism arises in which the exciton is clothed by virtual phonons whereas the phonons are dressed by virtual excitonic transitions. Therefore quantum decoherence occurs because dressed phonons and free phonons evolve differently. First, the exciton modifies the nature of the phonon quantum states through the dressing effect. As a result, a dynamical exciton-phonon entanglement occurs giving rise to a true decoherence according to the nomenclature of Joos[27]. Then, the exciton favors a renormalization of the phonon frequency so that the exciton coherences exhibit a phase factor that involves the frequency difference between free and dressed phonons. At finite temperature, an average is required because the phonons are assumed to be initially in thermal equilibrium. This average yields a sum over phase factors which interfere with the others resulting in the decay of the exciton coherence. This effect corresponds to the fake decoherence defined by Joos[27].

In this paper, a new facet of the exciton-phonon model is addressed via the introduction of a third ingredient. Indeed, assuming that the phonons are initially thermalized suggests that they correspond to an open system coupled with its own environment. For describing this situation, we use a simple model known in the literature as quantum Langevin theory (QLT)[41–45]. We thus introduce a thermal bath formed by an infinite number of harmonic oscillators that represent a true reservoir for the phonons. Note that such a situation is quite common. For instance, in most adsorbed nanowires, the vibrons are coupled with the phonons of the wire, these phonons interacting with a harmonic bath formed by the substrate vibrations[16]. In α-helices, amide-I vibrons are coupled with the phonons that refer to H-bond vibrations. The thermalization of these phonons can be described by using the QLT that accounts for their coupling with the remaining degrees of freedom of the protein[46]. Finally, optical spectroscopy in the condensed phase is usually addressed by considering a two-level system coupled with a finite number of primary nuclear coordinates that interact with a bath of

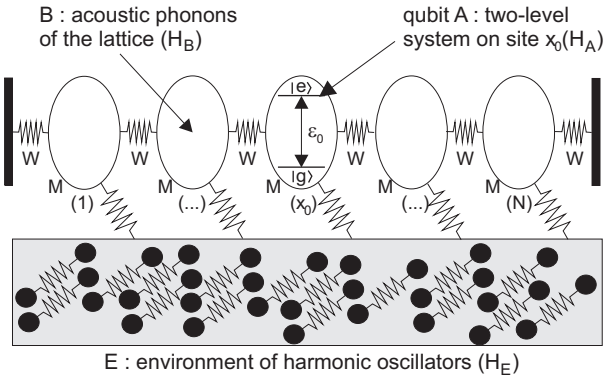

FIG. 1: Representation of the system involving a qubit A coupled with the phonons B of a finite-size lattice that interact with a thermal bath of harmonic oscillator E.

harmonic vibrations[47].

In that context, the fundamental question arises whether the harmonic bath affects the excitonic decoherence through its interaction with the phonons. Because it forces the phonons to thermalize, does the bath modify the exciton-phonon entanglement? Does the interplay between true and fake decoherence change when the phonons are allowed to relax over a bath? To partially answer these questions, we introduce a simple model in which the exciton is localized so that its dynamics is described by a two-level system. We aim to study the decoherence of such a qubit[48–50] when it interacts with confined phonons that are coupled with a harmonic bath. The most complex situation in which the exciton delocalizes will be addressed in forthcoming works.

The paper is organized as follows. In Sec. II, the system formed by the qubit, the confined phonons and the bath of harmonic oscillators is introduced. The corresponding Hamiltonians are defined. Then, the decoherence factor of the qubit is defined and evaluated. In Sec. III, numerical calculations are carried out for describing the time evolution of the decoherence factor whose behavior is discussed and interpreted.

II. THEORETICAL BACKGROUND

A. Model Hamiltonians

As illustrated in Fig. 1, we consider a one-dimensional lattice that contains N sites $x = 1, ..., N$. Each site is occupied by an atomic subunit whose internal dynamics is described by a two-level system. Neglecting interactions between neighboring internal degrees of freedom, we focus our attention on the x_0th two-level system. It defines a qubit A whose ground state $|g\rangle$ and first excited state $|e\rangle$ generate the Hilbert space $\mathcal{E}_A$. The qubit Hamiltonian is expressed in terms of the Bohr frequency ϵ_0 as (in unit $\hbar = 1$)

$$H_A = \epsilon_0 |e\rangle\langle e|. \tag{1}$$

The qubit interacts with the acoustic phonons B of the lattice. The phonons are the elementary excitations associated to the external motions of the lattice sites that behave as point masses M connected via force constants W. They refer to N normal modes with quantized wave vectors $q_p = p\pi/L$, with $p = 1, .., N$ and $L = N + 1$, and eigenfrequencies $\Omega_p = \Omega_c \sin(q_p/2)$ ($\Omega_c = \sqrt{4W/M}$). In the phonon Hilbert space $\mathcal{E}_B$, the phonon Hamiltonian is written in terms of the phonon operators $a_p^\dagger$ and a_p as

$$H_B = \sum_{p=1}^{N} \Omega_p a_p^\dagger a_p. \tag{2}$$

The qubit-phonon interaction results from the stochastic modulation of the qubit Bohr frequency by the lattice vibrations. Within the so-called potential deformation model, this effect is usually addressed by assuming that the coupling depends linearly on the phonon coordinates[24,25]. Here, we go beyond this approximation and we assume that the qubit Bohr frequency depends both linearly and quadratically on the lattice distortions[51–57]. In normal mode representation, the qubit-phonon coupling Hamiltonian is thus written as

$$V_{AB} = \sum_{p=1}^{N} \left\{ M_p (a_p^\dagger + a_p) + \delta\Omega_p a_p^\dagger a_p \right\} |e\rangle\langle e|, \tag{3}$$

where

$$\begin{aligned} M_p &= \Delta_0 \sqrt{\frac{8\Omega_p}{L\Omega_c}\left(1 - \frac{\Omega_p^2}{\Omega_c^2}\right)} \cos\left(\frac{p\pi x_0}{L}\right) \\ \delta\Omega_p &= \Delta_1 \frac{2\Omega_p}{L\Omega_c}\left[\cos^2\left(\frac{p\pi x_+}{L}\right) + \cos^2\left(\frac{p\pi x_-}{L}\right)\right], \end{aligned} \tag{4}$$

with $x_\pm = x_0 \pm 1/2$ and where Δ_0 (resp. Δ_1) is the strength of the linear (resp. quadratic) qubit-phonon coupling. Note that Eq.(3) is the simplest quantum nondemolition interaction that allows the description of fake decoherence which results from exciton-induced phonon frequency shift. When the coupling depends linearly on the phonon coordinates, such a shift arises only when the exciton is allowed to move[29–32]. To recover this feature with a localized exciton, it is thus necessary to introduce an additional interaction that depends quadratically on the phonon coordinates.

Finally, the phonons are coupled with additional vibrational modes. Each mode is described by a harmonic oscillator with frequency ω_α and boson operators b_α and $b_\alpha^\dagger$. These normal modes define a thermal bath E, whose Hamiltonian H_E acts in the Hilbert space $\mathcal{E}_E$, as

$$H_E = \sum_\alpha \omega_\alpha b_\alpha^\dagger b_\alpha. \tag{5}$$

According to the QLT[41–45], the bath favors energy exchanges mediated by the creation or the destruction of

phonons. Within the rotating wave approximation[41,42], the coupling Hamiltonian is defined as

$$V_{BE} = \sum_{\alpha p} g_{\alpha p} a_p^\dagger b_\alpha + g_{\alpha p}^* b_\alpha^\dagger a_p, \tag{6}$$

where $g_{\alpha p}$ is the strength of the coupling between the pth phonon mode and the αth oscillator.

The whole system involving a qubit coupled with confined phonons that interact with a harmonic bath is described by the Hamiltonian $H = H_A + H_B + H_E + V_{AB} + V_{BE}$. The Hilbert space $\mathcal{E} = \mathcal{E}_A \otimes \mathcal{E}_B \otimes \mathcal{E}_E$ is partitioned into independent subspaces as $\mathcal{E} = \mathcal{E}_g \otimes \mathcal{E}_e$, where $\mathcal{E}_g$ is the zero-exciton subspace (qubit in the ground state) whereas $\mathcal{E}_e$ is the one-exciton subspace (qubit in the excited state). Within this nomenclature, H can be rewritten as

$$H = \mathscr{H}_g \otimes |g\rangle\langle g| + (\mathscr{H}_e + \Delta\mathscr{H}) \otimes |e\rangle\langle e|, \tag{7}$$

where

$$\begin{aligned} \mathscr{H}_g &= \sum_{p=1}^{N} \Omega_p a_p^\dagger a_p + \sum_\alpha \omega_\alpha b_\alpha^\dagger b_\alpha + V_{BE} \\ \mathscr{H}_e &= \sum_{p=1}^{N} \hat{\Omega}_p a_p^\dagger a_p + \sum_\alpha \omega_\alpha b_\alpha^\dagger b_\alpha + V_{BE} \\ \Delta\mathscr{H} &= \sum_{p=1}^{N} M_p (a_p^\dagger + a_p). \end{aligned} \tag{8}$$

At this step, let $s = B + E$ be the system formed by the phonons and the harmonic bath. In Eqs.(7)-(8), $\mathscr{H}_g$ (resp. $\mathscr{H}_e$) governs the dynamics of s when the qubit lies in its ground state (resp. excited state). Note that $\mathscr{H}_e$ accounts for the renormalization of the phonon frequency $\hat{\Omega}_p = \Omega_p + \delta\Omega_p$ induced by the excitation of the qubit whereas $\Delta\mathscr{H}$ is the linear qubit-phonon coupling.

B. Definition of the decoherence factor

Without any perturbation, the system is in thermal equilibrium at temperature T. The qubit, whose frequency satisfies $\omega_0 \gg k_B T$, occupies its ground state. By contrast, the harmonic oscillators form a bath whose properties are encoded in the density matrix $\rho_E = \exp(-\beta H_E)/Z_E$, Z_E being the bath partition function ($\beta = 1/k_B T$). According to the QLT[41–43], the bath yields the thermalization of the phonons that are described by the density matrix $\rho_B = \exp(-\beta H_B)/Z_B$, with Z_B the phonon partition function. As a result, the system density matrix is written as $\rho_{eq} = |g\rangle\langle g| \otimes \rho_s$ where $\rho_s = \rho_B \otimes \rho_E$.

To study the decoherence of the qubit, the system is brought in a configuration out of equilibrium. The qubit is prepared in a superposition of states $|\psi_A\rangle = c_g|g\rangle + c_e|e\rangle$. This step is assumed to be faster than the typical time evolution of s so that the initial system density matrix becomes $\rho(0) = |\psi_A\rangle\langle\psi_A| \otimes \rho_s$.

In that context, the properties of the qubit are encoded in the reduced density matrix $\sigma(t) = Tr_s[\rho(t)]$, where Tr_s is a partial trace over the system s. The coherence is the matrix element $\sigma_{eg}(t) = \mathscr{D}(t) e^{-i\epsilon_0 t} \sigma_{eg}(0)$, where $\mathscr{D}(t)$ defines the so-called decoherence factor as

$$\mathscr{D}(t) = Tr_s \left[\rho_s e^{i\mathscr{H}_g t} e^{-i(\mathscr{H}_e + \Delta\mathscr{H})t} \right] \tag{9}$$

$\mathscr{D}(t)$ is the central object of the present study. Its knowledge provides information on the ability of the qubit to maintain a superposition at time t despite its coupling with the phonons. The key point is that $\mathscr{D}(t)$ depends only on the dynamics of s. It characterizes the way the quantum evolution of s deviates from a free evolution when the qubit-phonon coupling switches on, an average over the initial state being performed. Because the phonons interact with their environment, $\mathscr{D}(t)$ cannot be calculated easily so that an approximate procedure is applied, as detailed in the next section.

C. Calculation of the decoherence factor

To evaluate $\mathscr{D}(t)$, the evolution operator that governs the dynamics of s when the qubit is excited is written as

$$e^{-i(\mathscr{H}_e + \Delta\mathscr{H})t} = e^{-i\mathscr{H}_e t} \; e_+^{-i\int_0^t dt_1 \Delta\mathscr{H}(t_1)}, \tag{10}$$

where e_+ is a positive time ordered exponential[44] and $\Delta\mathscr{H}(t) = e^{i\mathscr{H}_e t} \Delta\mathscr{H} e^{-i\mathscr{H}_e t}$. By inserting Eq.(10) in Eq.(9), it turns out that $\mathscr{D}(t)$ involves the product $\exp(i\mathscr{H}_g t)\exp(-i\mathscr{H}_e t)$. Of course, this product does not simplify when the phonons interact with the harmonic bath ($[\mathscr{H}_g, \mathscr{H}_e] \neq 0$). However, to simplify the discussion, we assume that the weak-coupling limit is reached so that the product becomes

$$e^{i\mathscr{H}_g t} e^{-i\mathscr{H}_e t} \approx e^{-i\delta\mathscr{H} t}, \tag{11}$$

where $\delta\mathscr{H} = \mathscr{H}_e - \mathscr{H}_g$.

As shown in Eq.(8), $\delta\mathscr{H} = \sum_p \delta\Omega_p a_p^\dagger a_p$ commutes with H_B, H_E, ρ_B and ρ_E. This feature allows the introduction of the effective density matrix defined as

$$\rho_B(t) = Z_B^{-1}(t) e^{-\beta H_B - i\delta\mathscr{H} t} \tag{12}$$

where

$$Z_B(t) = Tr_B e^{-\beta H_B - i\delta\mathscr{H} t}. \tag{13}$$

Strictly speaking, $\rho_B(t)$ is not a phonon density matrix since it provides complex values for the population of the phonon number states. However, it reduces to the equilibrium density matrix ρ_B at $t = 0$. Moreover, $\rho_B(t)$ being isomorphic to ρ_B, the trace over the phonon degrees of freedom yields averages equivalent to thermal averages but with the correspondence $\beta\Omega_p \to \beta\Omega_p + i\delta\Omega_p t$.

Using the previous definitions, Eq.(9) is rewritten as

$$\mathscr{D}(t) \approx \frac{Z_B(t)}{Z_B} Tr_s \left[\rho_B(t)\rho_E e_+^{-i\int_0^t dt_1 \Delta\mathscr{H}(t_1)}\right] \quad (14)$$

In Eq.(14), it is as if the time was playing two different roles. In the evolution operator, t is the physical time during which the dynamics of s takes place. By contrast, in $\rho_B(t)$, t can be viewed as a parameter that characterizes the *initial* phonon state. Despite its arbitrariness, this distinction reveals that Eq.(14) is particularly suitable for using the cumulant expansion method[58,59]. Up to second order with respect to $\Delta\mathscr{H}$, this method yields

$$\begin{aligned}\mathscr{D}(t) \;\approx\; & \frac{Z_B(t)}{Z_B} e^{-i\int_0^t dt_1 m_1(t_1|t)} \\ & e^{-\int_0^t dt_1 \int_0^{t_1} dt_2 [m_2(t_1,t_2|t) - m_1(t_1|t)m_1(t_2|t)]},\end{aligned} \quad (15)$$

where the moments of $\Delta\mathscr{H}$ are expressed as

$$\begin{aligned} m_1(t_1|t) &= Tr_s\left[\rho_B(t)\rho_E \Delta\mathscr{H}(t_1)\right] \\ m_2(t_1,t_2|t) &= Tr_s\left[\rho_B(t)\rho_E \Delta\mathscr{H}(t_1)\Delta\mathscr{H}(t_2)\right]. \end{aligned} \quad (16)$$

According to Eq.(8), $m_1(t_1|t)$ and $m_2(t_1,t_2|t)$ involve the moments of the phonon operators that can be extracted from the QLT[41–43]. To proceed, the s dynamics is first defined in terms of coupled Heisenberg equations of motion for both the phonon operators and the bath operators. Then, these equations are formally integrated by invoking the Markov limit and the single-mode relaxation-time approximation (i.e. by neglecting the correlations between distinct phonon modes induced by the bath)[60]. The phonon dynamics is thus given by the Langevin equations of motion

$$\dot{a}_p^\mu(t) = i\mu(\hat{\Omega}_p + \delta_p)a_p^\mu(t) - \gamma_p a_p^\mu(t) + \mathscr{F}_p^\mu(t), \quad (17)$$

where $\mu = \pm$ (for $a_p^\dagger(t)$ and $a_p(t)$) and where $\mathscr{F}_p^\mu(t)$ is the Langevin force defined as

$$\mathscr{F}_p^\mu(t) = \sum_\alpha i\mu g_{\alpha p}^\mu e^{i\mu\omega_\alpha t} b_\alpha^\mu. \quad (18)$$

In Eq.(17), the phonon decay rate γ_p and the dynamical shift δ_p are defined as

$$\begin{aligned} \gamma_p &= \sum_\alpha \pi |g_{\alpha p}|^2 \delta(\hat{\Omega}_p - \omega_\alpha) \\ \delta_p &= p.v. \sum_\alpha \frac{|g_{\alpha p}|^2}{\hat{\Omega}_p - \omega_\alpha}, \end{aligned} \quad (19)$$

where $p.v.$ stands for the Cauchy principal value.

Eq.(17) yields $a_p^\mu(t)$ in terms of the integral of $\mathscr{F}_p^\mu(t)$. Therefore, using the fluctuation-dissipation theorem[43] that links the Fourier transform of the two-time correlation functions of the Langevin forces and the phonon decay rate, the moments of the phonon operators can be evaluated. First order moments vanish and the non-vanishing second order moments are defined as

$$\begin{aligned} & Tr_s\left[\rho_B(t)\rho_E a_p^\dagger(t_1)a_{p'}(t_2)\right] = \delta_{pp'} \times \\ & e^{i\tilde{\Omega}_p(t_1-t_2)} e^{-\gamma_p(t_1-t_2)} \left[\hat{n}_p + e^{-2\gamma_p t_2}(\bar{n}_p(t) - \hat{n}_p)\right], \end{aligned} \quad (20)$$

where $\tilde{\Omega}_p = \hat{\Omega}_p + \delta_p$, $\bar{n}_p(t) = [\exp(\beta\Omega_p + i\delta\Omega_p t) - 1]^{-1}$ and $\hat{n}_p = [\exp(\beta\hat{\Omega}_p) - 1]^{-1}$. Eq.(20) can be understood as follows. Initially, it is as if the phonons were described by the effective density matrix $\rho_B(t)$. Average phonon numbers are thus defined in terms of the effective distributions $\bar{n}_p(t)$. Then, according to the QLT, energy exchanges occur between the phonons and the harmonic bath. Because the bath is in thermal equilibrium, these exchanges favor the thermalization of the phonons. With a rate $2\gamma_p$, the pth phonon mode reaches a thermal equilibrium characterized by the Bose-Einstein distribution $\hat{n}_p$. This distribution accounts for the renormalization of the phonon frequency ($\hat{\Omega}_p = \Omega_p + \delta\Omega_p$) because the qubit lies in its excited state. In addition, the energy exchanges destroy the coherent nature of each phonon p that is characterized by a finite lifetime inversely proportional to γ_p. As a result, any two-time correlation function involving phonon operators irreversibly decreases with time.

After algebraic manipulations, $m_1(t_1|t)$ and $m_2(t_1,t_2|t)$ can be determined so that $\mathscr{D}(t)$ is finally written as

$$\mathscr{D}(t) \approx \frac{Z_B(t)}{Z_B} e^{-\Phi(t)}, \quad (21)$$

where $\Phi(t)$ is defined as

$$\begin{aligned} \Phi(t) &= \sum_p M_p^2[(2\hat{n}_p + 1)\mathscr{L}_{2p}(t) - i\mathscr{M}_{2p}(t)] \\ &+ \sum_p M_p^2(\bar{n}_p(t) - \hat{n}_p)[\mathscr{L}_{1p}^2(t) + \mathscr{M}_{1p}^2(t)]. \end{aligned} \quad (22)$$

The functions $\mathscr{L}_{ip}(t)$ and $\mathscr{M}_{ip}(t)$ are written as

$$\begin{aligned} \mathscr{L}_{ip}(t) &= \int_0^t dt_1 ... \int_0^{t_{i-1}} dt_i \cos(\tilde{\Omega}_p t_i) e^{-\gamma_p t_i} \\ \mathscr{M}_{ip}(t) &= \int_0^t dt_1 ... \int_0^{t_{i-1}} dt_i \sin(\tilde{\Omega}_p t_i) e^{-\gamma_p t_i}. \end{aligned} \quad (23)$$

Note that Eq.(21) is exact when the phonons do not interact with the harmonic bath ($V_{BE} = 0$).

According to standard theories[27,28], the decoherence factor measures how the phonon dynamics, perturbed by the qubit-phonon coupling that switches on when the qubit is excited, deviates from the free evolution that arises when the qubit occupies its ground state. This deviation has two origins because the coupling exhibits a linear contribution (denoted ℓ) and a quadratic contribution (denoted Q). The decoherence factor can thus be partitioned as $\mathscr{D}(t) = \mathscr{D}_Q(t)\mathscr{D}_\ell(t)$ with $\mathscr{D}_Q(t) = Z_B(t)/Z_B$ and $\mathscr{D}_\ell(t) = \exp(-\Phi(t))$.

Because of the quadratic coupling, the frequency of each phonon is shifted by an amount $\delta\Omega_p$ when the qubit is excited. Consequently, the reduced density matrix of the qubit exhibits a phase factor proportional to $\exp(-i\delta\mathscr{H}t)$. The phonons being initially in thermal equilibrium, the average of this phase factor according to the density matrix ρ_B gives rise to the so-called fake decoherence factor $\mathscr{D}_Q(t)$. Note that fake decoherence does not depend on the coupling between the phonons and the harmonic bath.

By contrast, the linear coupling $\Delta\mathscr{H}$ (Eq.(8)) affects the nature of the phonon quantum state. As described previously[35], it brings each phonon mode in a quasi-classical state that defines a lattice distortion localized on the site x_0. This distortion propagates so that two acoustic wave packets are emitted on each side of the excited site x_0. During their propagation, the wave packets experience reflections on the lattice sides and they relax over the harmonic bath. As a result, this quantum evolution differing from that which arises when the qubit is in its ground state, a dynamical qubit-phonon entanglement occurs *a priori* and a true decoherence takes place. The true decoherence factor $\mathscr{D}_\ell(t)$ is thus a measure of the phonon memory at time t of their initial distortion, this memory being encoded in the two-time correlation function of the linear coupling. Note that $\mathscr{D}_\ell(t)$ depends also on the quadratic qubit-phonon coupling. But the key point is that when compared with $\mathscr{D}_Q(t)$, $\mathscr{D}_\ell(t)$ strongly depends on the influence of the harmonic bath.

These different features are illustrated in the next section where the time evolution of the decoherence factor is studied numerically.

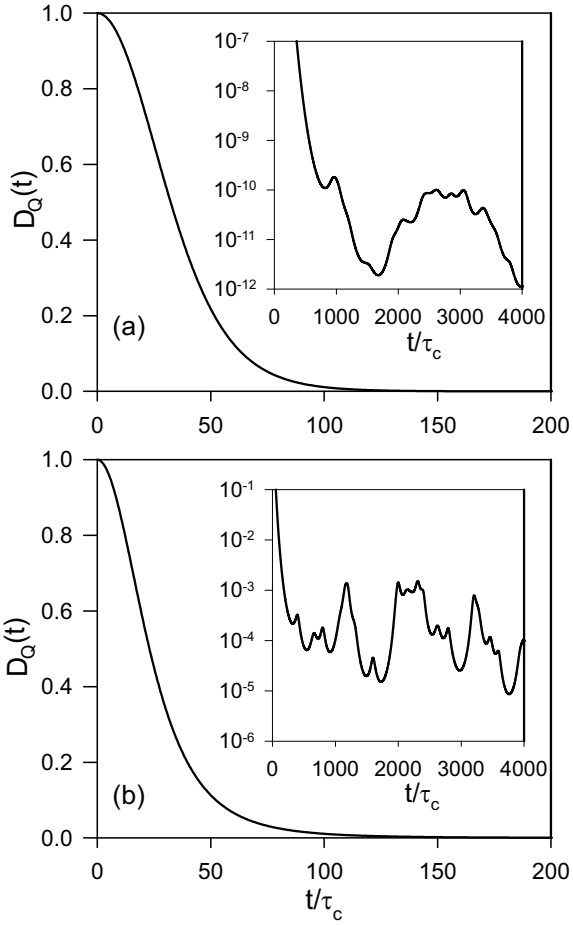

FIG. 2: Behavior of the fake decoherence factor $D_Q(t)$ for $\theta = 2.15$, $\Delta_Q = 1.66 \times 10^{-2}$, (a) $L = 20$ and (b) $L = 8$.

III. NUMERICAL RESULTS AND DISCUSSION

A. Parameters

In this section, the previous formalism is applied for describing the time evolution of the modulus $D(t) = |\mathscr{D}(t)|$ written as $D(t) = D_Q(t)D_\ell(t)$ with $D_Q(t) = |Z_B(t)/Z_B|$ and $D_\ell(t) = \exp(-Re[\Phi(t)])$ (see Eq.(21)). To proceed, we consider odd N values and assume that the qubit occupies the center of the lattice ($x_0 = L/2$). For describing the dynamics, the unit of time is the phonon correlation time $\tau_c = 2/\Omega_c$ and the reduced temperature $\theta = k_BT/\Omega_c$ is used. The strength of the linear and quadratic qubit-phonon couplings are measured by $\Delta_\ell = \Delta_0/\Omega_c$ and $\Delta_Q = \Delta_1/\Omega_c$, respectively. Finally, the interaction between the phonons and the bath is represented by a Debye model[1]. The decay rate γ_p scales as

$$\gamma_p = \frac{\gamma_0}{1 + \Omega_p^2/\omega_0^2} \tag{24}$$

with $\omega_0 = 10\Omega_c$ is the cutoff frequency of the bath. The strength of the coupling between the phonons and the bath is measured by the reduced parameter $\eta = \gamma_0/\Omega_c$. Note that δ_p is the Hilbert transform of γ_p.

B. Fake decoherence factor

The time evolution of the fake decoherence factor $D_Q(t)$ is displayed in Fig. 2 for $L = 20$ (Fig. 2a) and $L = 8$ (Fig. 2b). Initially equal to unity, $D_Q(t)$ decreases with time whatever L. It seems to follow a Gaussian decay and *a priori* vanishes in the long-time limit. In fact, we have verified that the behavior of $D_Q(t)$ is quite-well captured by its short-time limit. Consequently, from the expression of $Z_B(t)$ (Eq.(13)), $D_Q(t)$ scales as

$$D_Q(t) \approx \exp\left(-\frac{1}{2}\Gamma_Q^2 t^2\right) \tag{25}$$

where the decay rate Γ_Q is defined as

$$\Gamma_Q = \sqrt{\sum_p \Delta\bar{n}_p^2 \delta\Omega_p^2} \tag{26}$$

In Eq. (26), $\Delta\bar{n}_p^2 = \bar{n}_p(\bar{n}_p+1)$ measures the thermal fluctuations of the pth phonon number around its average value $\bar{n}_p = [\exp(\beta\Omega_p) - 1]^{-1}$. These fluctuations provide to Γ_Q its temperature dependence. Since $\bar{n}_p \approx k_BT/\Omega_p$ in the high-temperature limit, Γ_Q increases linearly with the temperature, as checked numerically. Moreover, Γ_Q depends on the quadratic qubit-phonon coupling through its dependence with respect to $\delta\Omega_p$. Because $\delta\Omega_p$ scales as $1/L$ (Eq.(4)), we have observed that the decay rate decreases with L as $\Gamma_Q \approx 2.4\Delta_Q k_BT/\sqrt{L}$. Fake decoherence is thus inherent to the confinement and it disappears in an infinite lattice.

Note that we must be careful because the isomorphism with the Gaussian strongly depends on the lattice size. Indeed, as illustrated in the insets of Fig. 2, $D_Q(t)$ shows coherence revivals. The shorter is L, the larger is the amplitude of the revivals. For instance, for $L = 20$, $D_Q(t)$ remains smaller than 10^{-10} indicating that the Gaussian approximation can be used. By contrast, for $L = 8$, $D_Q(t)$ reaches values approximately equal to 10^{-3} in the long-time limit. The Gaussian approximation breaks down and fake decoherence is incomplete.

C. True decoherence factor

Disregarding the coupling between the phonons and the harmonic bath, the time evolution of the true decoherence factor $D_\ell(t)$ is displayed in Fig. 3. When the quadratic qubit-phonon coupling vanishes (black line), $D_\ell(t)$ measures the phonon memory at time t of their initial perturbation induced by the linear qubit-phonon coupling (see Sec. II.C.). According to Eq.(22), it is defined as $D_\ell(t) = \exp(-\Phi_\ell(t))$ with

$$\Phi_\ell(t) = \sum_p M_p^2(2\bar{n}_p + 1)(1 - \cos(\Omega_p t)) \qquad (27)$$

Because of the confinement, the phonon dynamics exhibits quantum recurrences that provide to $D_\ell(t)$ an almost periodic nature characterized by several time scales. In the short-time limit (Fig. 3a), a series of dephasing-rephasing mechanisms occurs with an almost period $T_0 = L\tau_c$, i.e. the time required to the phonons to cover the lattice. Over half a period, the phonons deviate from their initial state so that dephasing takes place. The true decoherence factor decays[34] according to the rate $\Gamma_\ell \approx 8\Delta_\ell^2 k_BT$. Then, over the next half period, the phonons propagate back to the excited site so that they recover their initial state. The coherence of the qubit recurs resulting in a rephasing process that occurs with the same rate Γ_ℓ.

Over longer time scales (Figs. 3b and 3c), such a behavior remains. However, its periodic nature is more or less broken because the lattice dispersion prevents the phonon to recover their initial state after each reflection. Nevertheless, the dynamics is characterized by so-called revival times for which the initial state almost recurs.

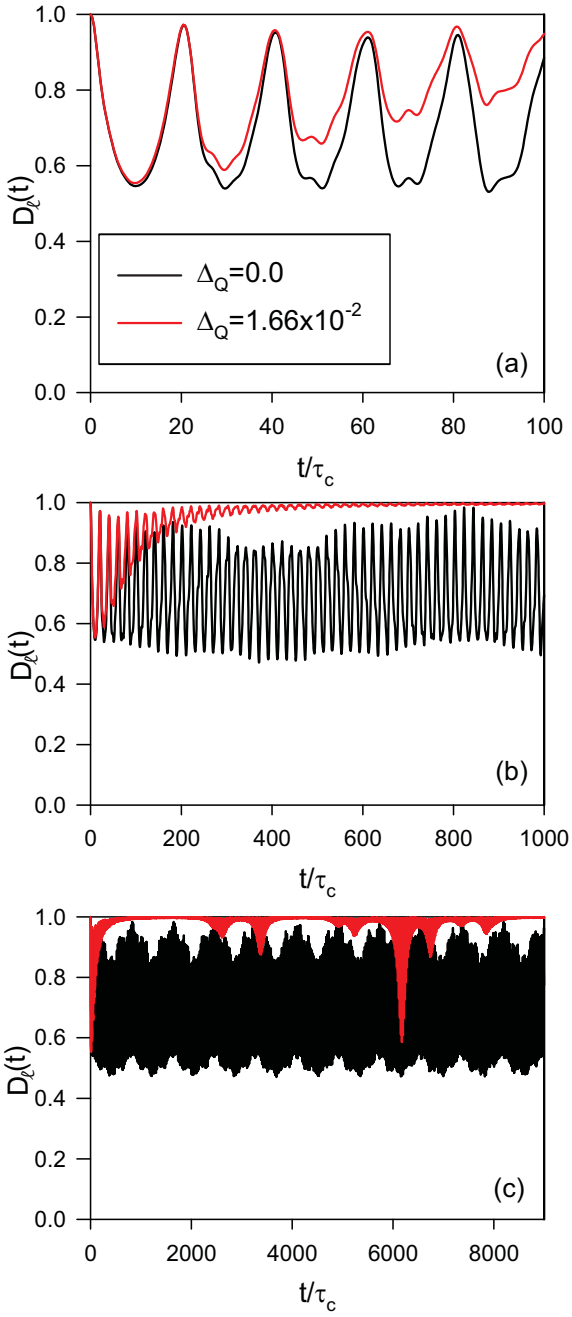

FIG. 3: Time evolution of the true decoherence factor $D_\ell(t)$ for $L = 20$, $\theta = 2.15$, $\Delta_\ell = 6.24 \times 10^{-2}$, and for $\Delta_Q = 0.0$ (black line) and $\Delta_Q = 1.66 \times 10^{-2}$ (red line). Different time scales are considered.

Here[34], this effect is encoded in the super-revival time $T_{sr} = L^3\tau_c/\pi^2$ equal to $810.56\tau_c$. Figs. 3b and 3c clearly show that $D_\ell(t)$ periodically recurs close to unity with a period approximately equal to T_{sr}.

At this step, let us mention that the strength of the linear qubit-phonon coupling discriminates between two asymptotic limits. In the weak-coupling limit ($\Gamma_\ell T_0 \ll 1$), the amplitude of the dephasing-rephasing process is small enough so that $D_\ell(t)$ basically remains close to

unity over an infinite time scale. By contrast, in the strong-coupling limit ($\Gamma_\ell T_0 \gg 1$), $D_\ell(t)$ clearly vanishes after a dephasing process and it recurs when the following rephasing mechanism takes place. However, it no longer reaches a value close to unity mainly because the lattice dispersion is enhanced by the coupling. Nevertheless, quantum recurrences occur periodically so that, as in the weak-coupling limit, the coherence of the qubit survives. In other words, when the phonons remain insensitive to the harmonic bath, there is no true decoherence in the sense that $D_\ell(t)$ does not vanish in the long-time limit. This mechanism will be named the incomplete true decoherence of the qubit.

The red curves in Fig. 3 show the influence of the quadratic qubit-phonon coupling on the true decoherence factor that becomes $D_\ell(t) = \exp(-\Phi_\ell(t))$ with

$$\Phi_\ell(t) = \sum_p M_p^2(2\bar{n}'_p(t)+1)(1-\cos(\hat{\Omega}_p t)) \qquad (28)$$

where $\bar{n}'_p(t) = Re(\bar{n}_p(t))$. When compared with the previous situation, it is as if the phonons were described by the effective density matrix $\rho_B(t)$ instead of ρ_B. Therefore, as shown in Fig. 3a, the dephasing-rephasing processes occur in the short-time limit, only. Over longer time scales (Fig. 3b), the oscillating behavior of the decoherence factor disappears gradually and after a time approximately equal to $125\tau_c$, $D_\ell(t)$ seems to reach a value quite close to unity. Nevertheless, as illustrated in Fig. 3c, quantum recurrences take place in the long-time limit resulting in the decay of $D_\ell(t)$ for specific revival times. This behavior originates in interference processes between the various contributions of the function $\Phi_\ell(t)$ (Eq.(28)). Indeed, $\bar{n}'_p(t)$ is a periodic function, with period $T_p = 2\pi/\delta\Omega_p$, that varies between $\bar{n}_p$ and $-1/2$ at high-temperature. Because each effective Bose number has its own period, interferences arise resulting in the decay of the function $\Phi_\ell(t)$. Over the decay time, we have verified that $\bar{n}'_p(t)$ behaves as a Gaussian whose decay rate, approximately equal to $\Gamma_Q/\sqrt{L}$, is almost p independent. Note that the recurrences observed in Fig. 3c correspond to specific periods T_p. For instance, with the parameters used in the simulation, one obtains $T_{p=2} = 6175\tau_c$ and $T_{p=4} = 3371\tau_c$ in a good agreement with the numerical observations.

Fig. 4 shows the influence of the coupling between the phonons and the harmonic bath on the time evolution of the true decoherence factor. The quadratic qubit-phonon coupling being neglected, the figure reveals the occurrence of two main effects.

First, because each phonon has a finite lifetime, the oscillating behavior of $D_\ell(t)$ gradually decays. This damping arises over a time scale approximately equal to $1/\gamma_0$ whose value discriminates between two regimes. The underdamped phonon regime arises when $\gamma_0 T_0 \ll 1$. In that case, the phonon lifetime is longer than the classical period T_0 so that the coherent nature of the phonons can be observed temporarily. Several dephasing-rephasing processes can be distinguished as illustrated by the black curve in Fig. 4. By contrast, the overdamped phonon regime takes place when $\gamma_0 T_0 \gg 1$. In that case, the phonon lifetime is shorter than the classical period T_0 preventing the observation of dephasing-rephasing processes (red curve). Note that the intermediate damped phonon regime occurs when $\gamma_0 T_0 \approx 1$.

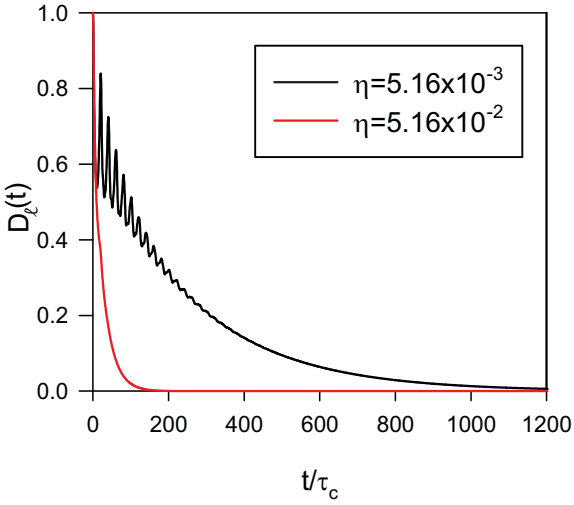

FIG. 4: Time evolution of the true decoherence factor $D_\ell(t)$ for $L = 20$, $\theta = 2.15$, $\Delta_\ell = 6.24 \times 10^{-2}$, $\Delta_Q = 0.0$ and for $\eta = 5.16 \times 10^{-3}$ (black line) and $\eta = 5.16 \times 10^{-2}$ (red line).

Second, because the phonon memory irreversibly disappears, $D_\ell(t)$ tends to zero in the long-time limit by following an exponential decay. In other words, the incomplete true decoherence becomes complete when the phonons are allowed to relax over the harmonic bath. From Eq.(22), one obtains $D_\ell(t) \approx \exp(-\Upsilon_\ell t)$ in the long-time limit, the decay rate Υ_ℓ being defined as

$$\Upsilon_\ell = \sum_p M_p^2(2\hat{n}_p+1)\frac{\gamma_p}{\tilde{\Omega}_p^2+\gamma_p^2} \qquad (29)$$

Note that when the quadratic qubit-phonon coupling and the phonon-bath coupling turn on, we have verified that the behavior of $D_\ell(t)$ results from the interplay between different processes. In a general way, a complete true decoherence arises and $D_\ell(t)$ vanishes in the long-time limit. However, over short and intermediate time scales, the damping of the dephasing-rephasing processes can result form either the phonon relaxation, the quadratic qubit-phonon coupling or both effects, depending on the values of the model parameters.

D. Full decoherence factor

The previous results reveal that the time evolution of $D_Q(t)$ and $D_\ell(t)$ is very sensitive to the model parameters. Consequently, different regimes were observed depending on the value of the following key ingredients: the fake decoherence rate Γ_Q, the dephasing-rephasing rate Γ_ℓ, the phonon decay rate γ_0 and the classical period T_0.

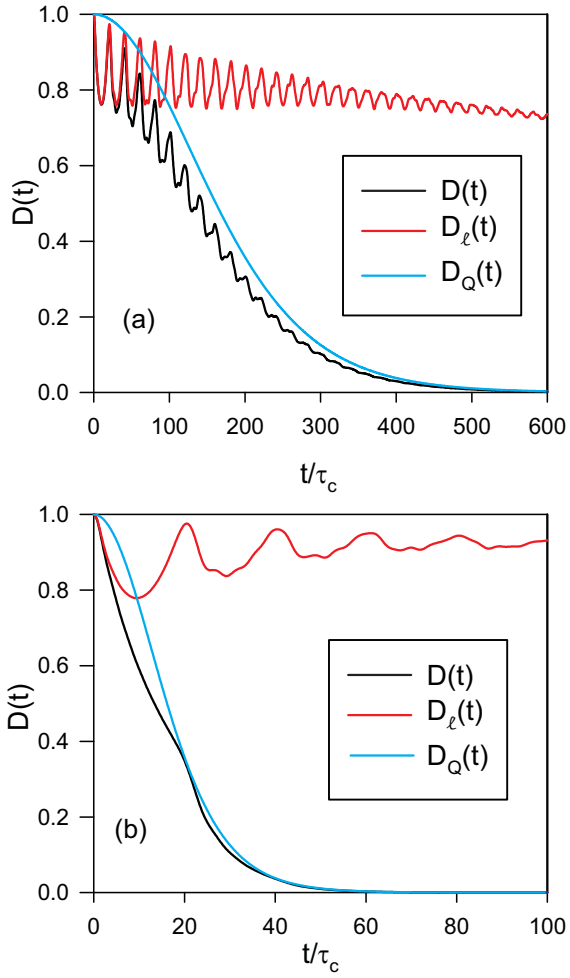

FIG. 5: Time evolution of the decoherence factor $D(t)$ for $L = 20$, $\theta = 2.15$, $\Delta_\ell = 4.16 \times 10^{-2}$, $\eta = 1.03 \times 10^{-3}$ and for (a) $\Delta_Q = 3.33 \times 10^{-3}$ and (b) $\Delta_Q = 3.33 \times 10^{-2}$.

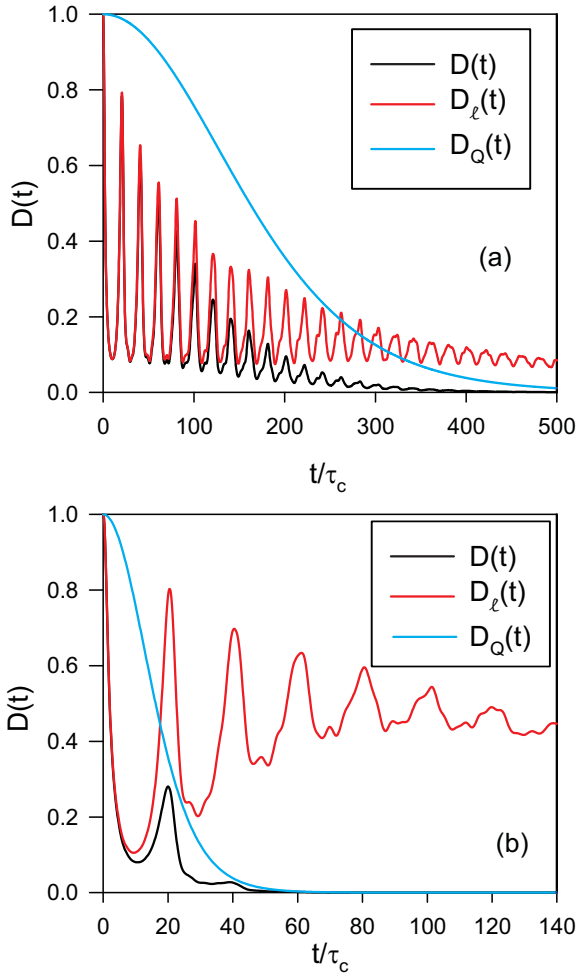

FIG. 6: Time evolution of the decoherence factor $D(t)$ for $L = 20$, $\theta = 2.15$, $\Delta_\ell = 1.25 \times 10^{-1}$, $\eta = 1.03 \times 10^{-3}$ and for (a) $\Delta_Q = 3.33 \times 10^{-3}$ and (b) $\Delta_Q = 3.33 \times 10^{-2}$.

In that context, because $D(t) = D_Q(t)D_\ell(t)$, one expects the occurrence of various time evolutions, as illustrated in the present section.

In the underdamped phonon regime ($\gamma_0 T_0 \ll 1$), the time evolution of $D(t)$ is shown in Fig. 5 when the linear qubit-phonon coupling remains weak (black curve). Note that $D_Q(t)$ (blue curve) and $D_\ell(t)$ (red curve) are also represented. For a weak quadratic qubit-phonon coupling (Fig. 5a), $D(t)$ follows a Gaussian decay that supports a high-frequency small-amplitude modulation. Indeed, in that case the coherent nature of the phonons can be distinguished so that a series of dephasing-rephasing processes arises. Because each dephasing is quite well compensated by the following rephasing, small-amplitude oscillations occur. They gradually disappear due to both the phonon relaxation and the interference effect induced by the quadratic qubit-phonon coupling. But this disappearance is quite slow so that fake decoherence dominates the decoherence process. $D(t)$ basically follows the Gaussian decay Eq.(25).

When the quadratic qubit-phonon coupling increases (Fig. 5b), $D(t)$ still follows a Gaussian decay but without the high-frequency small-amplitude modulation. In that case, fake decoherence occurs over a time scale shorter than the classical period T_0. Consequently, one cannot distinguish the dephasing-rephasing processes and $D(t)$ rapidly decays by following the Gaussian Eq.(25).

The time evolution of $D(t)$ is displayed in Fig. 6 for a stronger value of the linear qubit-phonon coupling (black curve). When the quadratic qubit-phonon coupling remains weak (Fig. 6a), $D(t)$ exhibits high-amplitude damped oscillations and vanishes in the long-time limit. Indeed, when Δ_ℓ increases, the amplitude of the dephasing-rephasing processes is enhanced. Over each cycle of duration T_0, an almost complete dephasing occurs that is no longer compensated by the following rephasing due to the lattice dispersion. Consequently, the degree of coherence of the qubit basically decreases with time. The key point is that there is no quantum recurrences because the incomplete true decoherence is observed over finite time scale Γ_Q^{-1} specified by the fake decoherence. This screening effect of the incomplete true

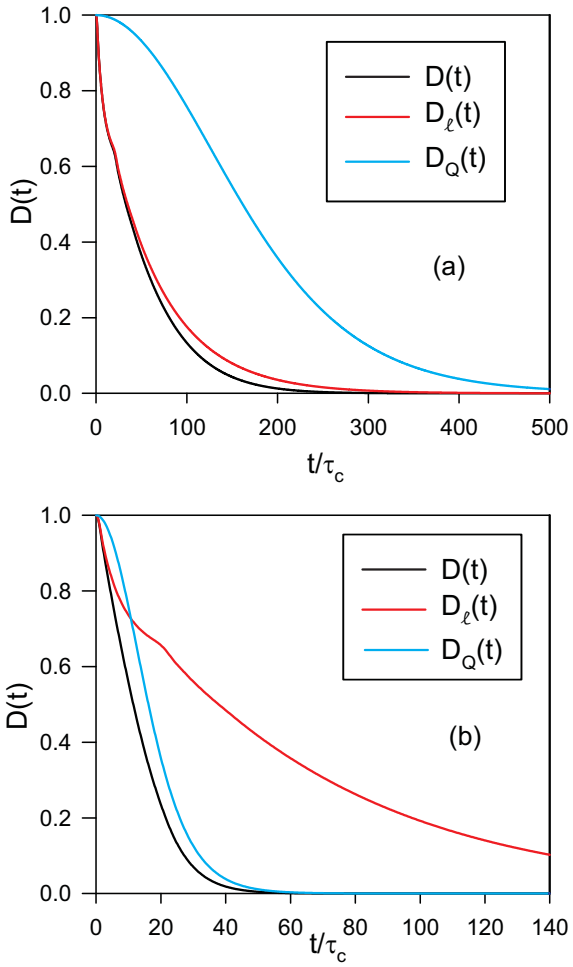

FIG. 7: Time evolution of the decoherence factor $D(t)$ for $L = 20$, $\theta = 2.15$, $\Delta_\ell = 4.16 \times 10^{-2}$, $\eta = 5.16 \times 10^{-2}$ and for (a) $\Delta_Q = 3.33 \times 10^{-3}$ and (b) $\Delta_Q = 3.33 \times 10^{-2}$.

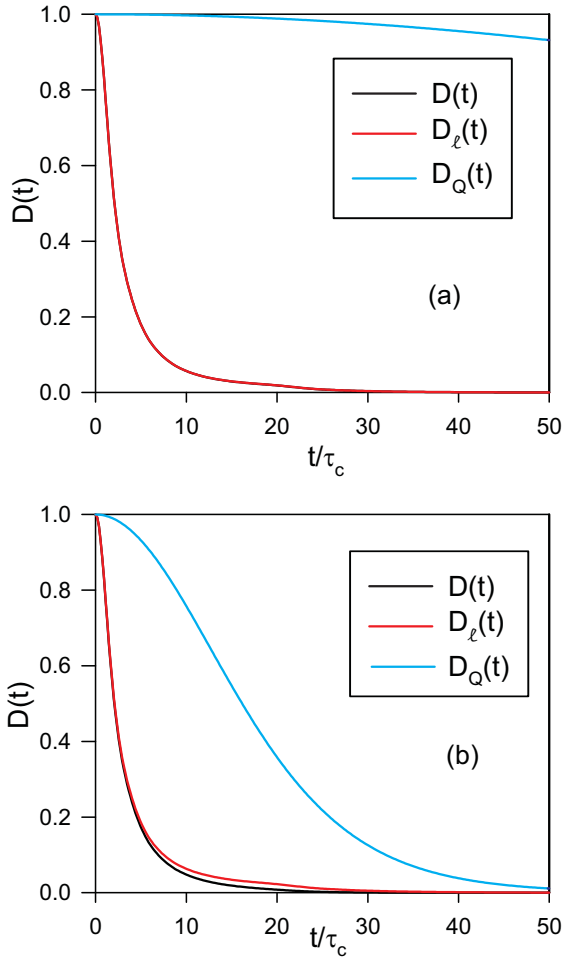

FIG. 8: Time evolution of the decoherence factor $D(t)$ for $L = 20$, $\theta = 2.15$, $\Delta_\ell = 1.25 \times 10^{-1}$, $\eta = 5.16 \times 10^{-3}$ and for (a) $\Delta_Q = 3.33 \times 10^{-3}$ and (b) $\Delta_Q = 3.33 \times 10^{-2}$.

decoherence induced by the fake decoherence ensures the completeness of the full decoherence.

When the quadratic qubit-phonon coupling increases (Fig. 6b), $D(t)$ rapidly decays and no longer supports high-frequency oscillations. Indeed, because Δ_Q increases, the temporal windows during which the incomplete true decoherence is monitored is drastically reduced. The fast decay of $D(t)$ originates in the strong screening induced by the Gaussian law of fake decoherence. It thus becomes almost impossible to distinguish any dephasing-rephasing process. Note that the fake decoherence selects the first dephasing process that basically refers to the dephasing-limited coherent dynamics that arises in an infinite lattice[35].

In the overdamped phonon regime ($\gamma_0 T_0 \gg 1$), the time evolution of $D(t)$ is displayed in Fig. 7 when the linear qubit-phonon coupling remains weak (black curve). In that regime, the phonon lifetime is shorter than the classical period T_0. The coherent nature of the phonons cannot be distinguished and one no longer observes the dephasing-rephasing processes. For a weak quadratic qubit-phonon coupling (Fig. 7a), $D(t)$ basically follows an exponential decay and it vanishes in the long-time limit. Such a behavior results from the fact that the rate Υ_ℓ, that controls the time evolution of the true decoherence factor, is larger than the decay rate Γ_Q so that fake decoherence can be disregarded. The decoherence of the qubit is thus dominated by the true decoherence whose completeness is ensured by the relaxation of the phonons over the harmonic bath.

When the quadratic qubit-phonon coupling increases, the opposite situation takes place as illustrated in Fig. 7b. Indeed, Γ_Q becomes larger than Υ_ℓ so that the time evolution of $D(t)$ is dominated by fake decoherence. Although $D(t)$ follows $D_\ell(t)$ in the short-time limit, it than decreases according to the Gaussian law of fake decoherence in the intermediate- and long-time limit.

The time evolution of $D(t)$ is displayed in Fig. 8 for a stronger value of the linear qubit-phonon coupling (black curve). When the quadratic qubit-phonon coupling remains weak (Fig. 8a), $D(t)$ explicitly follows the exponential decay that governs the time evolution of the true

decoherence factor. The figure clearly shows that such a behavior does not depend on fake decoherence. In fact, increasing Δ_ℓ results in the enhancement of the complete true decoherence. One thus obtains $\Upsilon_\ell \gg \Gamma_Q$ so that $D(t) \approx \exp(-\Upsilon_\ell t)$.

When the quadratic qubit-phonon coupling increases, Fig. 8b shows that the physics of the decoherence is almost unchanged. The rate Υ_ℓ remains larger than Γ_Q so that the complete true decoherence dominates the behavior of the full decoherence factor that is independent on fake decoherence. Of course, increasing again Δ_Q will result in a competition between true and fake decoherence. But it should be careful to not consider unphysical values.

At this step, note that to simplify the discussion, only specific asymptotic behaviors were reported in the present section. Of course, many other regimes occur between the underdamped phonon regime and the overdamped phonon regime, depending on the strength of the qubit-phonon coupling and on the value of the interaction between the phonons and the bath.

To conclude, let us mention that the previous results strongly depend on the lattice size via the L dependence of both the classical period T_0 and the fake decoherence rate Γ_Q. As L varies, one can pass from one regime to another. For instance, let us imagine that the parameters yield the underdamped phonon regime with weak linear and quadratic qubit-phonon couplings, as illustrated in Fig. 5a. As L increases, $\Gamma_\ell T_0$ is enhanced so that it is as if Δ_ℓ increased. In the same time, $\Gamma_Q T_0$ increases as if Δ_Q increased. One thus reaches the underdamped phonon regime with strong linear and quadratic qubit-phonon couplings, as illustrated in Fig. 6b. Note that we have verified that the influence of the size is less pronounced in the overdamped phonon regime provided that the phonon lifetime is shorter than the classical period T_0.

IV. CONCLUSION

In this paper, a simple model was introduced for studying the decoherence of a qubit coupled with the phonons of a finite-size lattice. Because of the confinement, the phonons no longer behave as a reservoir so that they remain sensitive to the excitation of the qubit. Consequently, the origin of the decoherence is twofold. First, the qubit modifies the phonon quantum states so that a dynamical qubit-phonon entanglement occurs giving rise to an incomplete true decoherence. Second, the qubit renormalizes the phonon frequency resulting in fake decoherence when a thermal average is realized. To account for the initial thermalization of the lattice, the phonons were viewed as an open system coupled with its own environment. To proceed, the quantum Langevin theory was applied by considering a thermal bath of harmonic oscillators over which the phonons can relax. It has been shown that the finite lifetime of the phonons does not modify the fake decoherence. By contrast, it strongly affects the incomplete true decoherence whose completeness finally arises. Therefore, the interplay between fake and true decoherence yields a very rich dynamics with various regimes, depending on the values of the model parameters.

Two asymptotic behaviors were reported in the present study. In the underdamped phonon regime, the phonon lifetime is *a priori* sufficiently long to observe the coherent nature of the confined phonons. For a weak linear qubit-phonon coupling, the decoherence of the qubit is dominated by fake decoherence. Therefore, $D(t)$ follows a Gaussian decay with or without small-amplitude oscillations, depending on the strength of the quadratic qubit-phonon coupling. For a strong linear coupling, the decoherence results from the screening of the incomplete true decoherence induced by fake decoherence. The coherent behavior of the phonons can be observed, depending on the quadratic coupling. In the overdamped phonon regime, the short phonon lifetime prevents the observation of the coherent nature of the confined phonons. The incomplete true decoherence disappears to the detriment of a complete true decoherence, the completeness resulting from the phonon relaxation. For a weak linear qubit-phonon coupling, the decoherence of the qubit ranges between complete true decoherence for a weak quadratic coupling, and fake decoherence for a strong quadratic coupling. By contrast, for a strong linear coupling, the decoherence is clearly independent on fake decoherence. Of course, many other regimes occur between these two asymptotic limits, depending on both the interaction between the phonons and the bath, and the strength of the qubit-phonon coupling.

* Electronic address: vincent.pouthier@univ-fcomte.fr

[1] V. May and O. Kuhn, *Charge and Energy Transfer Dynamics in Molecular Systems* (Wiley, Berlin, 2000).
[2] V. Agranovich, *Excitations in Organic Solids* (Oxford University Press, New York, 2009).
[3] E.R. Bittner, *Quantum Dynamics : Applications in Biological and Material Systems* (Taylor and Francis/CRC Press, New York, 2009).
[4] V. Sundstrom, Prog. Quantum Electron. **24**, 187 (2000).
[5] Th. Renger, V. May, and Oliver Kuhn, Phys. Rep. **343**, 137 (2001).
[6] E. Y. Poliakov, V. Chernyak, S. Tretiak, and S. Mukamel, J. Chem. Phys. **110**, 8161 (1999).
[7] C. Supritz, A. Engelmann, and P. Reineker, J. Lum. **119-120**, 337 (2006).
[8] R. H. Friend et al., Nature (London) **397**, 121 (1999).
[9] H. Tamura, E.R. Bittner, and I. Burghardt, J. Chem. Phys. **126**, 021103 (2007); **127**, 034706 (2007).
[10] A.C. Scott, Phys. Rep. 217, 1 (1992).
[11] W. Forner, Int. J. Quant. Chem. 64, 351 (1997).

[12] L. Cruzeiro, J. Chem. Phys. **123**, 234909 (2005).
[13] D. Tsivlin, H.-D. Meyer, and V. May, J. Chem. Phys. **124**, 134907 (2006).
[14] V. Pouthier, Phys. Rev. E **78**, 061909 (2008).
[15] D. Cevizovic, S. Galovic, and Z. Ivic, Phys. Rev. E **84**, 011920 (2011).
[16] B.N.J. Persson, Phys. Rev. B **46**, 12701 (1992).
[17] M. Bonn M, C. Hess, and M. Wolf, J. Chem. Phys. **115**, 7725 (2001).
[18] P. Jakob, J. Chem. Phys. **114**, 3692 (2001).
[19] V. Pouthier, C. Girardet, and J. C. Light, J. Chem. Phys. **114**, 4955 (2001).
[20] W.G. Roeterdink, O. Berg, and M. Bonn, J. Chem . Phys. **121**, 10174 (2004).
[21] C. Falvo and V. Pouthier, J. Chem. Phys. **122**, 014701 (2005).
[22] V. Pouthier, Phys. Rev. B **85**, 214303 (2012).
[23] V. Pouthier, J. Phys.: Condens. Matter **24**, 445401 (2012).
[24] H. Fröhlich, Adv. Phys. **3**, 325 (1954).
[25] T. Holstein, Ann. Phys. (N.Y.) **8**, 325 (1959); **8**, 343 (1959).
[26] S.M. Barnett and S. Stenholm, Phys. Rev. A **64**, 033808 (2001).
[27] E. Joos, H.D. Zeh, C. Kiefer, D. Giulini, J. Kupsch, and I.O. Stamatescu, *Decoherence and the Appearance of a Classical World in Quantum Theory* (Springer, New York, 2003).
[28] M. Schlosshauer, *Decoherence and the Quantum-to-Classical Transition* (Spinger Verlag, Berlin, 2007).
[29] V. Pouthier, Phys. Rev. B **83**, 085418 (2011).
[30] V. Pouthier, J. Chem. Phys. **134**, 114516 (2011).
[31] V. Pouthier, J. Chem. Phys. **137**, 114702 (2012).
[32] V. Pouthier, J. Chem. Phys. **138**, 044108 (2013).
[33] M. Esposito and P. Gaspard, Phys. Rev. E **68**, 066112 (2003).
[34] V. Pouthier, Phys. Rev. E **81**, 031913 (2010).
[35] V. Pouthier, J. Phys. : Condens. Matter **22**, 385401 (2010).
[36] H.P. Breuer, Phys. Rev. A **75**, 022103 (2007).
[37] C.R. Willis and R.H. Picard, Phys. Rev. A **9**, 1343 (1974).
[38] K.H. Hughes, C.D. Christ, and I. Burghardt, J. Chem. Phys. **131**, 024109 (2009).
[39] Y. Tanimura, J. Phys. Soc. Jpn. **75**, 082001 (2006).
[40] J. S. Jin, X. Zheng, and Y. J. Yan, J. Chem. Phys. **128**, 234703 (2008).
[41] W.H. Louisell, *Quantum Statistical Properties of Radiation* (Wiley, New York, 1973).
[42] C. Cohen-Tannoudji, J. Dupont-Roc, and G. Grynberg, *Atoms-Photon Interactions: Basic Processes and Applications* (Wiley, New York, 1992).
[43] N. Pottier, *Nonequilibrium Statistical Physics* (Oxford University Press, New York, 2010).
[44] S. Mukamel, *Principles of Nonlinear Optical Spectroscopy* (Oxford University Press, New York, 1995).
[45] A. O. Caldeira and A. J. Leggett, Physica A **121**, 587 (1983); Ann. Phys. **149**, 374 (1983).
[46] H. Freedman, P. Martel, and L. Cruzeiro, Phys. Rev. B **82**, 174308 (2010).
[47] Y. Tanimura and S. Mukamel, in *Ultrafast Dynamics of Chemical Systems*, edited by J. D. Simon (Kluwer, Dordrecht, 1994), p.327.
[48] A. Galindo and M. A. Martin-Delgado, Rev. Mod. Phys. **74**, 347 (2002).
[49] L.A. Openov, Phys. Lett. A **372**, 3476 (2008).
[50] R. Doll, P. Hanggi, S. Kohler, and M. Wubs, Eur. Phys. J. B **68**, 523 (2009).
[51] A. Nitzan and B. N. J. Persson, J. Chem. Phys. **83**, 5610 (1985).
[52] B. N. J. Persson and R. Ryberg, Phys. Rev. B **32**, 3586 (1985); Phys. Rev. Lett. **54**, 2119 (1985).
[53] P. Jakob and B. N. J. Persson, Phys. Rev. B **56**, 10644 (1997); Phys. Rev. Lett. **78**, 3503 (1997).
[54] D. Hsu and J.L. Skinner, J. Chem. Phys. **81**, 1604 (1984); **81**, 5471 (1984).
[55] D. Hsu and J.L. Skinner, J. Chem. Phys. **83**, 2097 (1985); **83**, 2107 (1985).
[56] D. Hsu and J.L. Skinner, J. Phys. Chem. **90**, 4931 (1986).
[57] V. Chernyak and S. Mukamel, J. Chem. Phys. **114**, 10430 (2001).
[58] R. Kubo, J. Phys. Soc. Jpn. **17**, 1100 (1962).
[59] J.H. Freed, J. Chem. Phys. **49**, 376 (1968).
[60] G.P. Srivastava, *The Physics of Phonons* (Hilger, New York, 1990).